Two-line atomic fluorescence flame thermometry using diode lasers

J. Hult*, I.S. Burns, C.F. Kaminski

Department of Chemical Engineering, University of Cambridge, Pembroke Street, Cambridge CB2 3RA, UK

Abstract

This paper reports on the first application of diode laser based LIF for pointwise temperature measurements in flames. The technique is based on two-line atomic fluorescence (TLAF) thermometry of indium atoms seeded at trace levels into the flame. Two novel extended cavity diode laser systems (ECDLs) were developed, providing tunable single-mode radiation around 410 and 451 nm, respectively, to excite the temperature sensitive $5P_{1/2}$–$6S_{1/2}$ and $5P_{3/2}$–$6S_{1/2}$ transitions of indium. The wide tuning range of the ECDLs allowed scans over the entire pressure broadened hyperfine structure of both transitions to be performed with signal-to-noise ratios exceeding 50 on single wavelength sweeps (at 20 Hz). We present a modified TLAF detection scheme that requires only a single detector and obviates the need for detection system calibration. Spatially resolved temperature profiles were obtained from a laminar premixed CH_4/air flame and found to be in excellent agreement with temperatures obtained from high-resolution OH LIF scans. The accuracy and spatial resolution of the technique makes this an attractive alternative to traditional, more complex, and expensive, temperature measurement techniques of similar or better precision. Finally, we demonstrate that PLIF imaging of atom distributions in flames is possible using low power diode lasers.
© 2004 The Combustion Institute. Published by Elsevier Inc. All rights reserved.

Keywords: Diode laser; LIF; Thermometry; Two-line atomic fluorescence; Premixed flame

1. Introduction

High-resolution temperature data of combustion processes are crucial for the development of combustion models and the characterisation of industrial combustion devices. The optical techniques developed for this purpose [1,2], e.g., Rayleigh and Raman scattering, coherent anti-Stokes Raman scattering (CARS), and laser induced fluorescence (LIF), have traditionally required the use of expensive and bulky systems, suffering

moderate to low spectral resolution and shot-to-shot intensity variations. In the last decade, however, compact diode lasers have emerged and found extensive use for measurements based on absorption techniques [3–6]. Their practicality derives from their compactness, robustness, their high-spectral purity, and their rapid tunability. Furthermore, they can be much cheaper than conventional laser systems (by as much as a factor of 1000), and thus have the potential to become much more widely used in research than any other laser type has hitherto been. Near-infrared diode lasers have found the most widespread application due to the robust technology available in the near-IR wavelength region. They have been

* Corresponding author. Fax: +44 1223 334796.
  E-mail address: jfh36@cheng.cam.ac.uk (J. Hult).

successfully used for absorption based flame temperature measurements, probing reactants such as O_2 [7], fuels such as C_2H_4 [8], product species such as H_2O [5,6], or seeded species such as caesium [9].

However, absorption based techniques suffer from poor spatial resolution because they are line-of-sight techniques, and this severely limits their use as temperature sensors for non-homogeneous or turbulent flows. Spatial averaging over regions of high and low temperatures results in distorted population distributions, from which accurate temperature information cannot be extracted unless a priori knowledge of the flow composition is available, which is rarely the case. Recently, diode lasers operating in the blue spectral region have become available [10–12], and are capable of direct excitation of electronic transitions of flame species. We have recently shown that such lasers can be successfully used for high-resolution LIF spectroscopy in flames [13]. Here, we report on the development of a new, high-precision flame temperature measurement technique based on two-line atomic fluorescence (TLAF) of atomic indium.

The paper is organised as follows: in Section 2, we review concepts of TLAF and proceed to present our TLAF scheme, which is much less calibration intensive than the one usually employed. In Section 3, the experimental details are presented. High-resolution scans of the indium hyperfine structure in the 5P–6S system are presented in Section 4. Spatially resolved temperature profiles from a laminar Bunsen flame are presented and compared to temperatures obtained from high-resolution OH LIF scans. Finally, we show PLIF images of indium distributions obtained with diode lasers and compare them to OH PLIF images. Conclusions and a future outlook are given in Section 5.

2. Theory

In TLAF, the population distribution of two temperature sensitive electronic states of atoms seeded into the flame is probed by measuring the Stokes and anti-Stokes direct-line fluorescence from a common upper state. Temperatures are then evaluated from the ratio of the corresponding fluorescence signals [14–17]. TLAF is an attractive measurement technique because it is not affected by molecular collisions: since excitation is to the same upper state for both fluorescence processes, quenching rates cancel out in the expression for temperature. Furthermore, atomic tracers have much higher transition strengths than molecular species, and thus lower excitation powers may be used. Indium is particularly suitable as a tracer for TLAF, because the spin–orbit splitting in the 5P ground state of indium leads to an energy spacing that is ideally matched to kT in typical combustion environments (1000–3000 K), leading to very high-temperature sensitivities [18,19]. Early demonstrations of the technique in flames employed lamps for excitation [15,18,20]. High-repetition rate pointwise temperature measurements in flames have been reported, employing two argon ion laser pumped continuous-wave dye lasers [17,21]. Our group has developed the method into a 2D thermometry approach [22] employing pulsed lasers, and reported the first application of the technique to map out cycle resolved 2D temperature profiles in a running SI prototype car engine [18,23].

Previous applications of indium TLAF were performed using two lasers and two detectors, as shown in the scheme depicted in Fig. 1A. In the diagram, the $5^2P_{1/2}$, $5^2P_{3/2}$, and the $6^2S_{1/2}$ levels are represented by numbers 1, 2, and 3, respectively. Initially, the $1 \rightarrow 3$ transition is pumped at λ_{31}, and the filtered fluorescence F_{32} is detected. Then, the $2 \rightarrow 3$ transition is pumped at λ_{32}, and F_{31} is detected using a second filtered detector. From the ratio of the two fluorescence signals, the temperature, T, can then be determined using Eq. (1). This equation can be derived by combining the rate equations with the Boltzmann population equation [14,17]

$$T = \frac{\Delta E/k}{\ln\left(\frac{F_{32}/I^v_{13}}{F_{31}/I^v_{23}}\right) + 4\ln\left(\frac{\lambda_{32}}{\lambda_{31}}\right) + \ln(C_1)}. \quad (1)$$

Here, I^v_{23} and I^v_{13} are the laser irradiances at λ_{32} and λ_{31}, respectively, ΔE is the energy separation between levels 1 and 2, and k is Boltzmann's constant. Note that no quenching rates appear in Eq. (1). Furthermore, due to the symmetry of the excitation and detection scheme, transition strengths also cancel out. C_1 is a non-dimensional calibration constant, which is determined experimentally and accounts for the varying efficiencies of the two detectors, transmission characteristics of filters, corrections for relative laser power measurements, and, in the case of multi-mode laser sources (not applicable here), the spectral overlap between the laser profile and the atomic transition. The calibration of relative detection efficiencies is usually the largest source of systematic error.

In this study, however, a different scheme is employed, using only a single detector, as shown in Fig. 1B. Excitation from level 1 to level 3 is still followed by detection of $3 \rightarrow 2$ fluorescence, denoted here by F_a. However, $2 \rightarrow 3$ excitation is
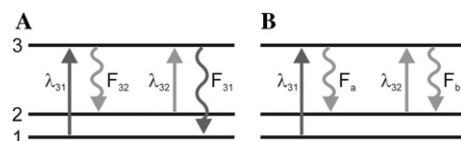

Fig. 1. (A) Conventional TLAF scheme and (B) modified TLAF scheme used in this study.

now followed by resonance fluorescence detection, F_b. This has the advantage that only one detector is needed, since both signals are now detected at λ_{32}. Of course, the technique would also work if one detects resonance fluorescence in the $3 \rightarrow 1$ transition instead [16], but there are several reasons why we prefer the former: the oscillator strength of the $3 \rightarrow 2$ transition at 451 nm is nearly twice as strong as the $3 \rightarrow 1$ transition ($A_{32} = 1.02 \times 10^8$ s^{-1}, $A_{31} = 0.56 \times 10^8$ s^{-1}). Furthermore, lower flame emission is present at 451 nm, and there is less fluorescence trapping for the signal at λ_{32} due to the lower population of state 2 compared to that of state 1. Our scheme obviates the need for calibration of differences in detection efficiencies, which hampers the previous approach. The resulting expression for temperature is now found to be:

$$T = \frac{\Delta E/k}{\ln\left(\frac{F_a/I_{13}^v}{F_b/I_{23}^v}\right) + 3\ln\left(\frac{\lambda_{32}}{\lambda_{31}}\right) + \ln\left(\frac{A_{32}}{A_{31}}\right) + \ln(C_2)}.$$

(2)

A disadvantage compared with the previous approach is that the Einstein coefficients, A_{31} and A_{32}, now appear explicitly and need to be known. In this scheme, the experimental calibration constant C_2 includes only small corrections, for example for the calibration of the laser power detector efficiencies at λ_{31} and λ_{32}, which can be measured. It is worth noting that, since resonance fluorescence is observed for F_b, our technique is applicable only in open flames with low particulate loading.

3. Experiment

Two novel widely tunable extended cavity diode lasers operating around 410 and 451 nm

were designed, which are described in [13,24]. Fabry–Perot GaN laser diodes (Nichia), without anti-reflection coatings, were mounted in Littrow cavities to achieve tunable single-mode radiation [25]. Each cavity consisted of the diode, a collimating aspheric lens, and a holographic 1800 lines/mm grating attached to a piezo-actuated kinematic mount [24,26]. The injection current and temperature of the diodes were controlled by standard laser driver units (Tektronix, LDC8002 and TED 8020). The output powers of the 410 and 451 nm ECDLs were 3.2 and 1.0 mW, respectively. By simultaneous tuning of diode current and piezo voltage, mode-hop free tuning ranges exceeding 90 GHz were achieved, at scanning rates of 20 Hz.

The experimental set-up for TLAF thermometry is illustrated in Fig. 2. The 410 and 451 nm beams were overlapped and combined using a dichroic mirror and focused using an $f = 300$ mm lens to a beam diameter of around 100 μm. The LIF signal was imaged at $f^\# = 2.4$ through a pinhole ($d = 150$ μm) onto a photomultiplier tube (Hamamatsu, R3788), resulting in a probe volume of around $0.1 \times 0.1 \times 0.15$ mm^3. An interference filter centred around 451.1 nm (CVI, $\Delta\lambda = 3$ nm) was used to suppress flame emission. The laser powers were continuously recorded by monitoring reflections from quartz plates using photodiodes. The wavelength scans of the two lasers were monitored using a solid low finesse quartz etalon ($FSR = 3.1$ GHz) in transmission mode. Laser powers were referenced using a calibrated laser power meter, inserted after the focusing lens. In the interaction region, the power in the 451 nm beam was 0.4 mW. The power in the 410 nm beam was attenuated to 0.2 mW at the same location, in order to achieve fluorescence signals of similar intensities for the two transitions. The saturation irradiances of both transitions were theoretically estimated to ensure that the experiments were
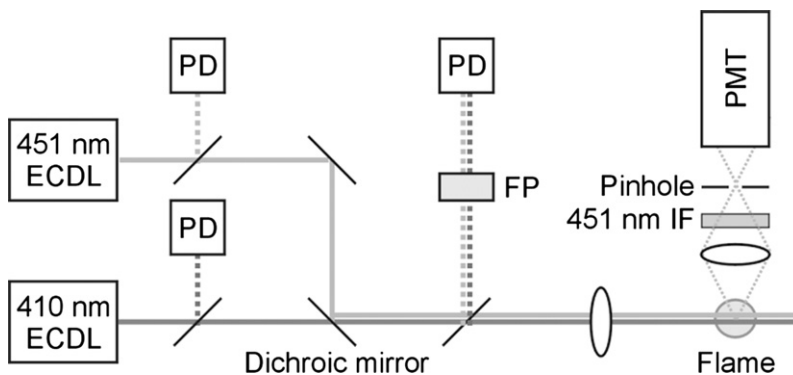

Fig. 2. Schematic illustration of experimental set-up used (ECDL, extended cavity diode laser; PD, photo diode; FP, Fabry–Perot etalon; IF, interference filter; and PMT, photomultiplier tube).

performed in the linear excitation regime. The calculation was done for a three-level system [27] and the effects of collisional quenching and pressure broadening at the experimental conditions were accounted for. For both excitation wavelengths, irradiances were found to be below saturation limits. The linear proportionality between the laser power and fluorescence signal strength was also experimentally confirmed for both transitions using a variable beam attenuator. The ECDLs were controlled and synchronised using a digital function generator. The LIF signal, laser power signals, and the etalon trace were all digitised by a 16 bit data acquisition card (National Instruments PCI-6014).

The spectra were divided by the laser power and averages of 200 spectra were used for the evaluation of temperatures. Theoretical spectra were fitted to the averaged spectra using a non-linear least squares fitting routine. The fitted spectra were integrated to yield F_a/I_{13}^v and F_b/I_{23}^v, which were then used to evaluate temperatures according to Eq. (2).

An axis-symmetric premixed laminar CH_4/air Bunsen flame ($\phi \geqslant 1$) stabilised on a translatable burner with a diameter of 10 mm was used for this study. A pneumatic nebuliser was used to seed the airflow with a dilute solution of $InCl_3$ (10^{-2} mol/L) in distilled water (seeding rate: 2.5 ml/h). At this level of seeding, no direct absorption of the laser beams by indium atoms was detected by a photodiode after a single pass of the laser beam through the flame when scanning over either of the two transitions.

In a separate experiment, the output from the 410 nm ECDL was used for planar laser induced fluorescence measurements (PLIF) of the indium distribution in the laminar flame. For this purpose, the laser wavelength was fixed to the centre peak of the $5^2P_{1/2} \to 6^2S_{1/2}$ transition. The laser beam was expanded to a sheet with a cross-section of 15×0.1 mm^2. The PLIF signal was detected using a digital video camera equipped with a 451 nm interference filter. Exposure times of individual frames corresponded to 8 ms. Laser sheet inhomogeneities were compensated for by recording fluorescence from dilute dye solutions.

The TLAF temperatures were validated by OH excitation scans performed in the same burner. Here, the frequency doubled output from a Nd:YAG laser pumped dye laser was employed. The laser wavelength was scanned from 281.5 to 283.2 nm to excite rotational lines with $0.5 \leqslant J \leqslant 15.5$ in the (0, 1) vibrational band of the $A^2\Sigma^+ \leftarrow X^2\Pi$ system. OH fluorescence signals from the (0, 0) and (1, 1) bands were collected by a PMT filtered with a UG 11 and a WG305 filter. OH LIF spectra were simulated and fitted to the experimental spectra using a weighed non-linear least squares fitting routine, using the program

described in [28]. The program takes full account of rotational line dependence of the transition moment, fluorescence quantum yield (including effects of quenching and rotational energy transfer), and collisional broadening.

4. Results

The continuous single-mode tuning range of the ECDL systems allowed scanning of the laser wavelength over the entire width of both indium transitions, as shown in Fig. 3. The $5^2P_{1/2} \to 6^2S_{1/2}$ transition at 410 nm consists of four hyperfine components, the positions and strengths of which are indicated in Fig. 3A. Figure 3 shows an average spectrum of 200 single scan spectra, a single scan spectrum obtained in 50 ms, and a theoretical fit to the average spectrum. The theoretical spectrum is the best non-linear least squares fit of the experimental spectrum with position, intensity scaling factor, background offset, and Voigt broadening coefficient as floating parameters. Relative hyperfine peak separations were taken from the literature [29], and intensities were calculated from the respective Clebsch–Gordan coefficients [30].

The fitted Voigt profiles yield a pressure broadening component of around 6.6 GHz, assuming a a Doppler broadening component of around 2.2 GHz corresponding to a temperature of 2000 K. The pressure broadening coefficient is in good agreement with that expected for N_2 dominated collisional broadening at this temperature and pressure [31]. Note that the total width of the $5^2P_{1/2} \to 6^2S_{1/2}$ transition is observed to be around 30 GHz, which is considerably wider than what has previously been assumed (2 GHz [17]) and used in TLAF measurements. The observed width of this transition is thus comparable to or even larger than the line width of conventional dye laser systems. Effects of the temperature dependence of the spectral overlap between the laser profile and the transition line width must therefore be taken into consideration when designing such experiments. In the present technique, this is avoided since the it is possible to scan over the entire transition system at a much higher resolution (<10 MHz laser linewidth). Signal-to-noise ratios exceeding 50 were obtained even on single scan spectrum, demonstrating the potential of the technique for dynamic measurements. Note that the fluctuations observed on the single scan spectrum are mainly due to local fluctuations in the indium concentrations, which are observed to be largest close to the flame front. It should also be noted that the apparently higher noise levels observed on the right-hand side of the single scan spectrum are a normalisation artefact because laser powers diminished towards the end of the scan.
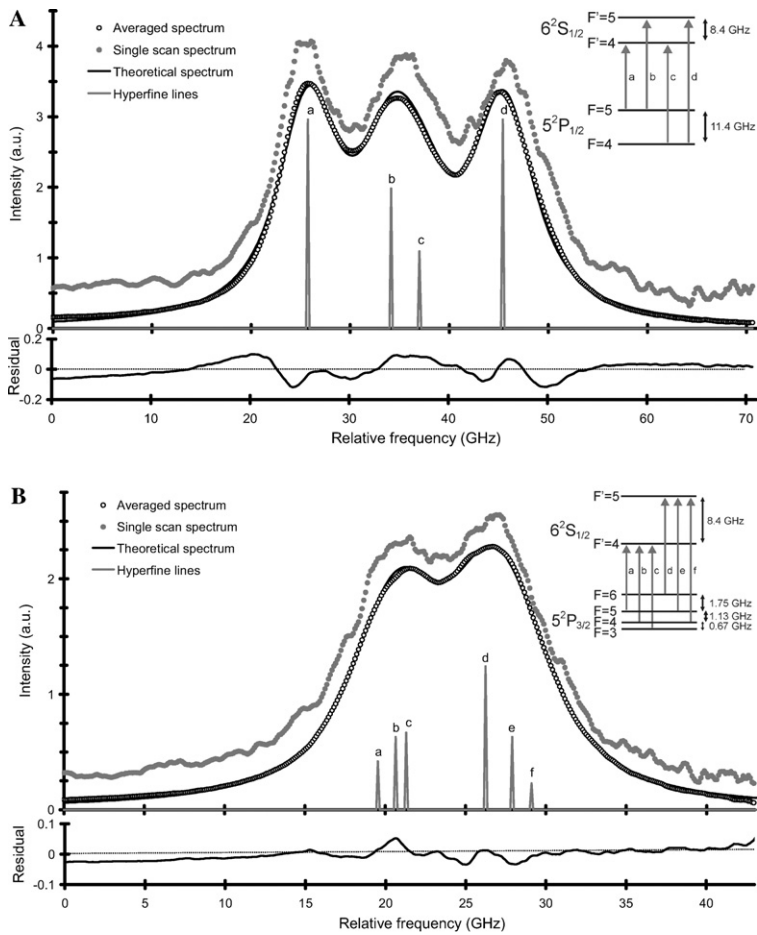
Fig. 3. Indium LIF spectra of: (A) the $5^2P_{1/2} \rightarrow 6^2S_{1/2}$ indium transition near 410 nm, and, (B) of the $5^2P_{3/2} \rightarrow 6^2S_{1/2}$ transition near 451 nm. Single scan spectrum is shown offset from the averaged spectra to improve clarity. Theoretical fits, residuals, and positions and relative strengths of individual hyperfine peaks are also shown. The insert shows details of the transitions involved.

Figure 3B shows the corresponding LIF excitation spectrum of the $5^2P_{3/2} \rightarrow 6^2S_{1/2}$ transition near 451 nm. This consists of six closely spaced hyperfine transitions, as indicated. A pressure broadening coefficient of 5.8 GHz was measured here, which is smaller than for the $5^2P_{1/2} \rightarrow 6^2S_{1/2}$ transition discussed earlier, but this is consistent with previous findings for other group III metals [32]. Note that background levels in the fit were close to zero, even for this resonance fluorescence spectrum.

Figure 4 shows vertical profiles of the 410 and 451 nm fluorescence signals along the centre axis of the flame. Data points correspond to the integrated fluorescence signal from 200 spectra, normalised by the laser power. At heights between 15.5 and 16 mm significant increases in the indium LIF signals are observed, as the neutral indium atoms are generated close to the flame front. The fluorescence signals then decrease gradually with increasing height, due to the oxidisation of
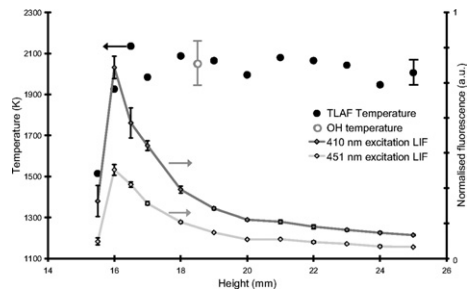

Fig. 4. Temperature and TLAF signals along a vertical axis through the centre of the flame. A temperature datum obtained from an OH excitation scan is also shown.

indium. Error bars shown correspond to the standard deviation of the integrated fluorescence powers obtained from single scans. Observed signal

variations are thought to stem from dynamic changes in neutral indium formation. This is substantiated by the fact that error bars are largest near the tip of the flame where neutral indium production rates are strongly affected by minute flame flicker.

The temperature profile, also shown in Fig. 4, was directly evaluated from averaged fluorescence powers using Eq. (2). The excellent spatial resolution demonstrates the superiority of TLAF over conventional line-of-sight absorption techniques to perform temperature measurement in spatially inhomogeneous combustion environments. A steep rise in temperature is seen near the flame front, with temperature staying nearly constant in the post-flame region, in agreement with previous studies of CH_4/air Bunsen flames [33]. Temperatures in the post-combustion region are seen to slightly fluctuate from one measurement point to the next (around 2.5%). This scatter is a consequence of both minor drifts in local indium concentration and small flame movements due to currents of ambient air and flow speed variations.

The largest systematic error in our temperature measurement arises from the calibration of laser power meters. We conservatively estimate this to be around 10% in our case, which would introduce a systematic uncertainty of 7% or 130 K at 2000 K. Further systematic errors stem from the uncertainty in reported A coefficients of the two indium transitions, uncertainties in the frequency calibration of laser scans, detector non-linearities, and background flame emission, but these are all much less significant in the present case. The error bar shown at $h = 25$ mm reflects the estimated total systematic uncertainty.

A reference temperature measurement, indicated by a grey circle, was made at $h = 18.5$ mm by performing an OH excitation scan. Figure 5 shows the corresponding excitation scan, together with the best fit simulated OH spectrum, giving a temperature of 2049 ± 110 K (for a detailed discussion of uncertainties associated with the current procedures see [28], in the present case it is a combination of both flame fluctuations and fitting accuracy). As seen, the agreement between TLAF and OH measurements is excellent. In principle, such independent measurement techniques
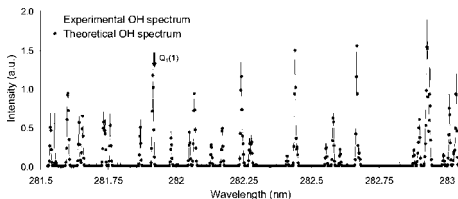
can be used to narrow down the systematic error mentioned in the previous paragraph. However, the small errors involved are a challenge even for the most accurate reported measurement techniques. For well-established temperature techniques, for example CARS, Raman or Rayleigh scattering accuracies as low as 1–2%, 2%, and 1%, respectively, have been reported in laminar flames [1,34]. There is no reason why the present technique should not achieve similar or better accuracies, however, a careful calibration of the laser power meters at the respective excitation wavelengths would then be required.

In Fig. 6, a horizontal TLAF temperature profile is shown, obtained at a height of 10 mm above the burner. Again a steep increase in the indium signal is observed as the flame front is crossed, although the drop in signal is not as drastic as in the corresponding vertical profile in Fig. 4. The temperature increase at the flame front is clearly captured, the maximum temperature is slightly lower along this profile compared to the maximum temperature of the vertical profile through the upper part of the flame, which is in agreement with previous findings [33].

Figure 7A shows a PLIF image of the indium distribution in the flame and Fig. 7B shows a corresponding OH PLIF image (imaged regions: 22×10 mm^2). The left-hand side is a composite image of four indium PLIF measurements obtained at different flame heights with 410 nm excitation. The OH PLIF corresponds to excitation of the $Q_1(1)$ line (indicated in Fig. 5) at 281.9 nm. Several observations can be made by comparing these two images. First note that excellent signal-to-noise ratios are obtained even with weak diode laser excitation, which offers promise for a future extension of the diode TLAF technique to a planar measurement technique. Second, there is an observed anti-correlation between regions of high-indium signals and high-OH signals. This is in correspondence with previous investigations of similar flames [35], where indium concentrations were found to be low in regions where strong oxidation takes place.

Fig. 5. OH excitation scan recorded at $h = 18.5$ mm. The fitted spectrum corresponds to a temperature of 2049 ± 110 K.
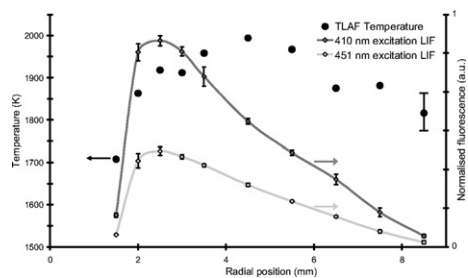

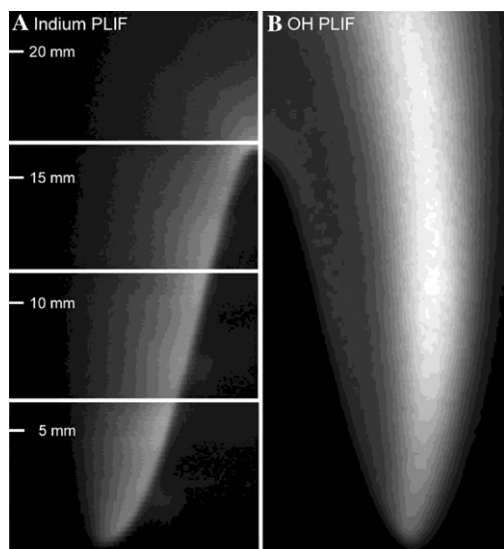Fig. 6. Temperature and TLAF signals along a horizontal axis through the centre of the flame.

Fig. 7. PLIF image of: (A) indium distribution and (B) OH distribution from a laminar premixed CH$_4$/air Bunsen flame.

5. Conclusions

This paper reports on the development of a novel temperature measurement technique based on two-line atomic fluorescence (TLAF) measurements with blue diode lasers. To the authors' knowledge, this is the first application of diode lasers for LIF based temperature measurements. The technique probes the relative population of two electronic states in indium atoms, which were seeded at trace levels to the flame. Two extended cavity diode lasers (ECDLs) operating near 410 and 451 nm were constructed. The ECDLs allowed rapid scanning of the entire pressure broadened hyperfine structure of the $5^2P_{1/2} \rightarrow 6^2S_{1/2}$ and $5^2P_{3/2} \rightarrow 6^2S_{1/2}$ transitions. Their width was measured to be 30 and 14 GHz, respectively, much larger than what had previously been reported in the literature.

A modified version of the TLAF technique was used, employing only a single detector and detection wavelength, obviating the need for a calibration of the signal collection system, which is the largest contribution to uncertainties in conventional TLAF. Spatially resolved temperature profiles of a laminar flame were measured, and obtained temperatures agreed well with those obtained by independently performed OH LIF excitation scans. Finally, the potential of using diode lasers for PLIF imaging of atomic species was demonstrated. Two-dimensional diode TLAF measurements may become a possibility in the future.

It has previously been reported that indium TLAF has potential as a tool for measurements in rich, sooting, flames where OH thermometry is not possible [22]. To apply TLAF in such systems, a two detector approach involving non-resonance fluorescence detection from each indium transition would be required to avoid interference from scattered laser radiation. The calibration constant C_1 in Eq. (1) required for such a measurement is efficiently obtained by first performing a measurement in a non-sooting flame using the single detector scheme described in the present paper followed by a measurement using the non-resonant, double detector scheme. Note that this does not require any modifications to the optical set-up.

Currently, we are modifying our present TLAF set-up to allow high-repetition rate measurements to be performed, which would enable the probing of turbulent flames. To do this, the diodes will no longer be operated in scanning mode because the ECDL wavelength tuning is not rapid enough. Instead, the laser lines will be locked to frequencies near the peaks of respective indium transitions. A rapid laser switching scheme similar to what has been outlined by Dec and Keller [17] could be envisaged to achieve kHz repetition rates. The blue diode laser TLAF technique offers exciting potential for a wide range of applications. Traditional temperature measurement techniques have suffered from the problems associated with high-power laser systems, such as pulse-to-pulse intensity and mode fluctuations, large laser line widths, and low repetition rates, which can be overcome with diode lasers.

References

[1] A.C. Eckbreth, *Laser Diagnostics for Combustion Temperature and Species*, second ed. Gordon & Breach, Amsterdam, Netherlands, 1996.
[2] J.W. Daily, *Prog. Energy Combust. Sci.* 23 (1997) 133–199.
[3] R.M. Mihalcea, D.S. Baer, R.K. Hanson, *Meas. Sci. Technol.* 9 (1998) 327–338.

[4] M.G. Allen, *Meas. Sci. Technol.* 9 (1998) 545–562.

[5] M.E. Webber, J. Wang, S.T. Sanders, D.S. Baer, R.K. Hanson, *Proc. Combust. Inst.* 28 (2000) 407–413.

[6] V. Ebert, T. Fernhoz, C. Giesemann, H. Pitz, H. Teichert, J. Wolfrum, H. Jaritz, *Proc. Combust. Inst.* 28 (2000) 423–430.

[7] S.T. Sanders, J. Wang, J.B. Jeffries, R.K. Hanson, *Appl. Opt.* 40 (2001) 4404–4415.

[8] L. Ma, S.T. Sanders, J.B. Jeffries, R.K. Hanson, *Proc. Combust. Inst.* 29 (2002) 161–166.

[9] S.T. Sanders, D.W. Mattison, L. Ma, J.B. Jeffries, R.K. Hanson, *Opt. Express* 10 (2002) 505–514.

[10] S. Nakamura, *Science* 281 (1998) 956–961.

[11] S. Nagahama, T. Yanamoto, M. Sano, T. Mukai, *Phys. Stat. Sol. A* 190 (2002) 235–246.

[12] H. Leinen, D. Gläßner, H. Metcalf, R. Wynands, D. Haubrich, D. Meschede, *Appl. Phys. B* 70 (2000) 567–571.

[13] J. Hult, I.S. Burns, C.F. Kaminski, *Opt. Lett.* 29 (2004) 827–829.

[14] C.Th. Alkemade, *Pure Appl. Chem.* 23 (1970) 73–97.

[15] N. Omenetto, P. Benetti, G. Rossi, *Spectrochim. Acta B* 27 (1972) 453–461.

[16] G. Zizak, N. Omenetto, J.D. Winefordner, *Opt. Eng.* 23 (1984) 749–755.

[17] J.E. Dec, J.O. Keller, *Proc. Combust. Inst.* 21 (1986) 1737–1745.

[18] H. Haraguchi, B. Smith, S. Weeks, D.J. Johnson, J.D. Winefordner, *Appl. Spectrosc.* 31 (1977) 156–163.

[19] J. Engström, C.F. Kaminski, M. Aldén, G. Josefsson, I. Magnusson, *1999 SAE International Congress and Exposition*. Society of Automobile Engineers, Warrendale, PA, 1999, Paper No. 1999-01-3541.

[20] G. Zizak, F. Cignoli, S. Benecchi, *Appl. Spectrosc.* 33 (1979) 179–182.

[21] R.G. Joklik, J.W. Daily, *Appl. Opt.* 21 (1982) 4158–4162.

[22] J. Engström, J. Nygren, M. Aldén, C.F. Kaminski, *Opt. Lett.* 25 (2000) 1469–1471.

[23] C.F. Kaminski, J. Engström, M. Aldén, *Proc. Combust. Inst.* 27 (1998) 85–93.

[24] I.S. Burns, J. Hult, C.F. Kaminski, *Appl. Phys. B* 79 (2004) 491–495.

[25] K.B. MacAdam, A. Steinbach, C. Wieman, *Am. J. Phys.* 60 (1992) 1098–1111.

[26] L. Ricci, M. Weidemüller, T. Esslinger, A. Hemmerich, C. Zimmermann, V. Vuletic, W. König, T.W. Hänsch, *Opt. Commun.* 117 (1995) 541–549.

[27] G. Zizak, J.D. Bradshaw, J.D. Winefordner, *Appl. Opt.* 19 (1980) 3631–3639.

[28] B. Atakan, J. Heinze, U.E. Meier, *Appl. Phys. B* 64 (1997) 585–591.

[29] G.V. Deverall, K.W. Meissner, G.J. Zissis, *Phys. Rev.* 91 (1953) 297–299.

[30] C. Candler, *Atomic Spectra and the Vector Model*. Hilger & Watts, London, 1964.

[31] J. Eberz, G. Huber, T. Kühl, G. Ulm, *J. Phys. B* 17 (1984) 3075–3082.

[32] B. Cheron, R. Scheps, A. Gallagher, *Phys. Rev. A* 15 (1977) 651–660.

[33] B.A.V. Benett, J. Fielding, R.J. Mauro, M.B. Long, M.D. Smooke, *Combust. Theory Model.* 3 (1999) 657–687.

[34] N.M. Laurendeau, *Prog. Energy Combust. Sci.* 14 (1988) 147–170.

[35] J. Nygren, J. Engström, J. Walewski, C.F. Kaminski, M. Aldén, *Meas. Sci. Technol.* 12 (2001) 1294–1303.

Comments

Igor Rahinov, Tel-Aviv University, Israel. The strong part of this work is that you eliminate the need to use 2 detectors and 2 filters by using excitation and detection on the same wavelength. However, it can be a main disadvantage, since the scattering, which cannot be filtered spectrally can cause an error in this 2-line technique. Can you give an estimation of such kind of error and comment on the possibility to use temporal separation of fluorescence from scattering, which will probably allow the use of this technique in highly scattering environments as well?

Reply. In the present study, all of the temperature measurements were performed in clean flames. It was not our intention to imply that the single-detector scheme should be used to make measurements in sooting or particle-laden flames. It is correct that scattering of incident laser light would compromise the fidelity of this resonance fluorescence method. However, the single-detector technique can be used in a clean flame to make reference temperature measurements from which a two-detector technique can be calibrated. The two-detector configuration, thus calibrated, could then be used to make measurements in particle-laden environments.

●

Joachim W. Walewski, University of Wisconsin-Madison, USA. In your work, you claim that the calibration constant, in the expression for the measured temperature is only dependent on "external" quantities, for example, spectral detector responsivity, filter transmission, etc. In reality, this factor also contains the convolution of both laser line profiles with the respective absorption line profiles. In your presentation you show that the absorption lines are dominated by pressure broadening. This makes the convolutions and thus the calibration constant a function of pressure. So if you want to apply your method in environments with varying pressure, e.g., internal-combustion engines or higher turbulent flames, you either need to scan over the absorption line in a time shorter than the time scale of a noticeable pressure change, or you would need to attain knowledge of the dependence of C on the pressure from "external" sources, e.g., from calibration measurements and the knowledge of the local pressure.

Reply. It is true that the shapes of the indium spectra are pressure dependent. All of the experiments described here, however, were performed at constant (atmo-

spheric) pressure. Furthermore, in the present study, the entire indium fluorescence spectra were acquired by scanning the wavelengths of the narrow linewidth diode lasers. The fluorescence strengths Fa and Fb, used to determine the temperature, represent the integrated areas under these spectra, and are thus independent of spectral shape. Therefore, for the work presented here, the calibration constant 'C' is not a function of pressure. We have mentioned the future possibility of making TLAF temperature measurements at high repetition-rates and applying the technique to dynamic combustion processes. It is not currently possible to scan the wavelengths of the blue extended-cavity diode lasers over the entire indium transitions at sufficiently high rates

for the study of such systems. A different approach would be to lock the laser lines to wavelengths near the centre of the indium transitions, and to switch between them on a time-scale that is much faster than the changes in temperature and pressure. In this case, the pressure would indeed have to be known at the measurement time, if the corresponding line-shape changes were appreciable, and if the pressure dependence of the two fluorescence signals was significantly different. One possibility to recover partial line-shape information quickly may be to modulate the laser frequency around a restricted region of the indium transition by tuning the diode injection current, while keeping the extended cavity fixed.